The Probe of Inflation and Cosmic Origins

A Space Mission Study Report
December, 2018

Principal Investigator:
Steering Committee:
Executive Committee:
Contributors:
Endorsers:

1 Executive Summary (2 pg, Hanany)

2 Science (31 pages)

48 pages are currently distributed as 29/19: 29 pages for science (including foregrounds and systematics), 19 for instrument, technology, mission, management and cost.

2.1 Introduction (1.5 pgs, Hanany + (?))

NASA suggested table of contents says Science Intro or Landscape section should include:

- State of the Art in the Field

- Compelling Outstanding Questions

- Needed Capabilities for Progress

2.2 Science Objectives (17.5 pgs)

The PICO Science Traceability Matrix (2pg, Hanany&Trangsrud) will be inserted around here. It is an 11x17 foldout, so it counts as 2 pages, which leaves 15.5 to all the rest in 2.2. Currently allocating 15 pages.

FOR EACH OF THE BELOW SUBSECTIONS:

- Introduce and elaborate on the applicable PICO "Science Objectives" from the STM table (what do they mean and why are they important)

- Observations/Measurements that enable PICO to accomplish each Science Objective (tell the data analysis story that connects the Observations column of the STM to the Science Objective column)

- Contextualize relative to sub-orbital and other space missions. *Emphasize where capabilities are unique to space.*

- Science yield estimate (be quantitative. how well will PICO do at Baseline/Required performance? at Current Best Estimate performance?)

- Include a summary plot or table which demonstrates PICO's performance against the Science Objective as written (e.g. how it discriminates between different theories)

- Perceived science impact. (The impact isn't reducing sigma on a parameter. It is about what we will learn about nature.)

2.2.1 Fundamental Physics (6 pgs, Flauger, Green)

To include: Cosmic Inflation, Particle Physics (Neutrinos and Light Relics), primordial EM fields Should address these Science Objectives from the STM:

- "Probe the physics of the big bang by detecting the energy scale at which inflation occurred if it is above 4×10^{15} GeV, or place an upper limit if it is below" [r]

- "Probe the physics of the big bang by excluding classes of potentials as the driving force of inflation" [n_s, n_{run}]

- "Determine the sum of neutrino masses, and distinguish between inverted and normal neutrino mass hierarchies" [Σm_ν]

- "Detect departures from or tightly constrain the thermal history of the universe" [N_{eff}]

- Origin of magnetic fields and cosmic birefringence

Gravitational waves and inflation

Measurements of the CMB together with Einstein's theory of general relativity imply that the observed density perturbations must have been created long before the CMB was released, and rather remarkably even before the universe became filled with a hot and dense plasma of fundamental particles. What generated these perturbations is one of the biggest questions in cosmology.

While the dynamics of the plasma produces some amount of gravitational waves, the amplitude is too small to be detected in existing or planned CMB experiments. So any imprint of gravitational waves on the cosmic microwave background detected by PICO would constitute evidence for gravitational waves from the same primordial period that created the density perturbations. Because the dynamics of gravitational waves is essentially unaffected by the plasma physics, they would be a pristine relic left over from the earliest moments of our universe, and their properties would shed light on the mechanism that created the primordial perturbations that grew into the anisotropies of the CMB and the stars and galaxies around us. Knowledge of the strength of the signal and their statistical properties would transform our understanding of many areas of fundamental physics.

Inflation, a period of nearly exponential expansion of the early universe, is the leading paradigm explaining the origin of the primordial density perturbations. It predicts a nearly scale invariant spectrum of primordial gravitational waves originating from quantum fluctuations. Thus, a detection of these gravitational waves would be the first detection of phenomenon associated with quantum gravity. Because the spectrum is scale-invariant, one may hope to detect primordial gravitational waves over a wide range of frequencies including, for example, at LIGO or LISA frequencies. However, as a consequence of the expansion of the universe, the energy density in the gravitational waves rapidly dilutes with increasing frequency, and observations of the CMB provide the easiest, and for the foreseeable future only way to detect these gravitational waves.

The strength of the signal, often quantified by the tensor-to-scalar ratio r, is a direct measure of the expansion rate of the universe during inflation. Together with the Friedmann equation, this reveals one of the most important characteristics of inflation, its energy scale. PICO will be able to detect primordial gravitational waves if inflation occurred at an energy scale of at least 4×10^{15} GeV. A detection would have profound implications for fundamental physics because it would provide evidence for a new energy scale, and would allow us to probe physics at energies far beyond the reach of terrestrial colliders.

The signal would have two contributions, one on degree angular scales or multipoles of $\ell \sim 80$, typically referred to as the recombination peak, and another contribution for multipoles of $\ell \lesssim 20$ from reionization. The contribution from reionization is expected to be strongest relative to the
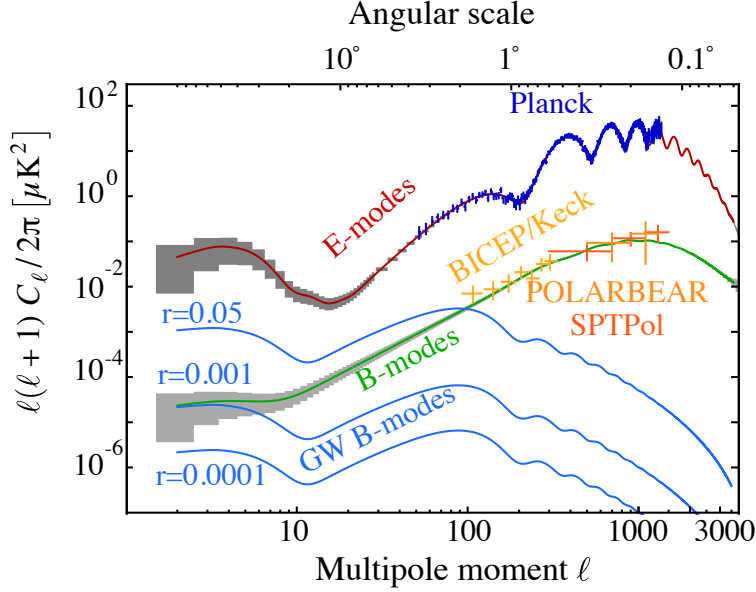
Figure 1: power spectrum place holder

contribution from weak lensing and instrumental noise. No sub-orbital experiment has meaningfully measured modes at $\ell < 40$ and a satellite like PICO is the most suitable approach to reach the lowest multipoles.

There are two classes of slow-roll inflation that naturally explain the observed value of the spectral index of primordial fluctuations, n_s. The first class is characterized by potentials of the form $V(\phi) \propto \phi^p$. This class includes many of of the simplest models of inflation, some of which have already been strongly disfavored by existing observations. If the constraints on the spectral index tighten by about a factor 2 with the central value unchanged, and the upper limits on r improve by an order of magnitude, this class would be ruled out.
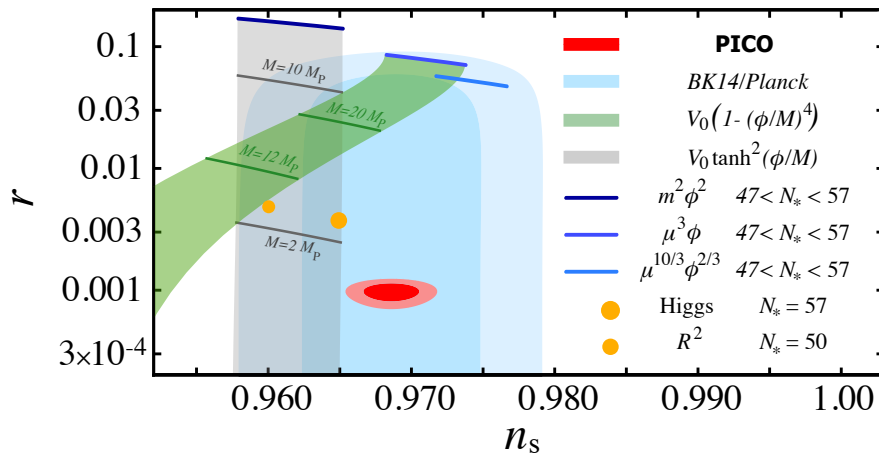

Figure 2: nsr placeholder

The second class is characterized by potentials that exponentially approach a plateau and include R^2 inflation. This model predicts a tensor-to-scalar ratio of $r \sim 0.003$. All models in this class with

a characteristic scale in the potential that is larger than the Planck scale predict a tensor-to-scalar ratio of $r \gtrsim 0.001$, and an experiment like CMB-S4 could exclude these scenarios. However, there are models such as the Goncharov-Linde model with a somewhat smaller characteristic scale that predict a tensor-to-scalar ratio of $r \sim 4 \times 10^{-4}$.

In the absence of a detection, PICO would limit the amount of gravitational waves to $r < 10^{-4}$ at 95% CL. This is stronger than current upper limits by three orders of magnitude, and stronger than those expected for the ground-based experiment CMB-S4 by an order of magnitude.

Models of inflation, or the early universe more generally, differ in their predictions for the scalar spectral index $n_{\rm s}$ and its scale dependence, often referred to as the running of the spectral index $n_{\rm run}$. With its high resolution and low noise levels, PICO will improve the constraints on $n_{\rm s}$ and $n_{\rm run}$ by a factor of about two. In addition, PICO will probe the statistical properties of the primordial fluctuations over a wide range of scales with exquisite precision and improve constraints on departures from Gaussianity by a factor $2 - 3$.

Light relics

In the inflationary paradigm, the universe was reheated to temperatures of at least 10 MeV and perhaps as high as 10^{12} GeV. At these high temperatures, even very weakly interacting or very massive particles, such as those arising in extensions of the standard model of particle physics, can be produced in large abundances [1, 2]. As the universe expands and cools, the particles fall out of equilibrium, leaving observable signatures in the CMB power spectra. Through these effects the CMB is a sensitive probe of neutrino and of other particles' properties.

One particularly compelling target is the effective number of light relic particle species $N_{\rm eff}$, also called the effective number of neutrinos. The canonical value with three neutrino families is $N_{\rm eff} = 3.046$. Additional light particles contribute a change to $N_{\rm eff}$ of $\Delta N_{\rm eff} \geq 0.027\,g$ where $g \geq 1$ is the number of degrees of freedom of the new particle [3, 4]. This defines a target of $\sigma(N_{\rm eff}) < 0.027$ for future CMB observations. Either a limit or detection of $\Delta N_{\rm eff}$ at this level would provide powerful insights into the basic constituents of matter.

Forecasts for $N_{\rm eff}$ are shown in Figure 3. The two most important parameters for improving constraints are the fraction of sky observed $f_{\rm sky}$ and the noise. Achieving both larger $f_{\rm sky}$ and lower noise are strengths of PICO compared to other platforms. Our baseline mission nearly reaches the target constraint with $g = 1$. A newly designed mission with only 10 times higher sensitivity will reach $\sigma(N_{\rm eff}) < 0.025$. A high precision measurement of the CMB in temperature and polarization is the only proven approach to reach this important threshold.

Many light relics of the early universe are not stable. They decay, leaving faint evidence of their past existence on other tracers. The relics with sufficiently long lifetime to survive few minutes, past the epoch of light element synthesis, leave a signature on the helium fraction Y_p. If they decay by the time of recombination, their existence through this period is best measured through the ratio of $N_{\rm eff}$ to Y_p. PICO's cosmic variance limited determination of the E mode power spectra will improve current limits for these quantities by a factor of five thus eliminating sub-MeV mass thermal relics.

Cosmological measurements have already confirmed the existence of one relic that lies beyond the Standard Model: dark matter. For a conventional WIMP candidate, the CMB places very stringent constraints on its properties through the signature of its annihilation on the T and E spectra [**? ? ?**]. *Planck* currently excludes WIMPs with mass $m_{\rm dm} < 16$ GeV and a future CMB mission could reach $m_{\rm dm} < 45$ GeV for $f_{\rm sky} = 0.8$. The CMB provides the most stringent constraints on the
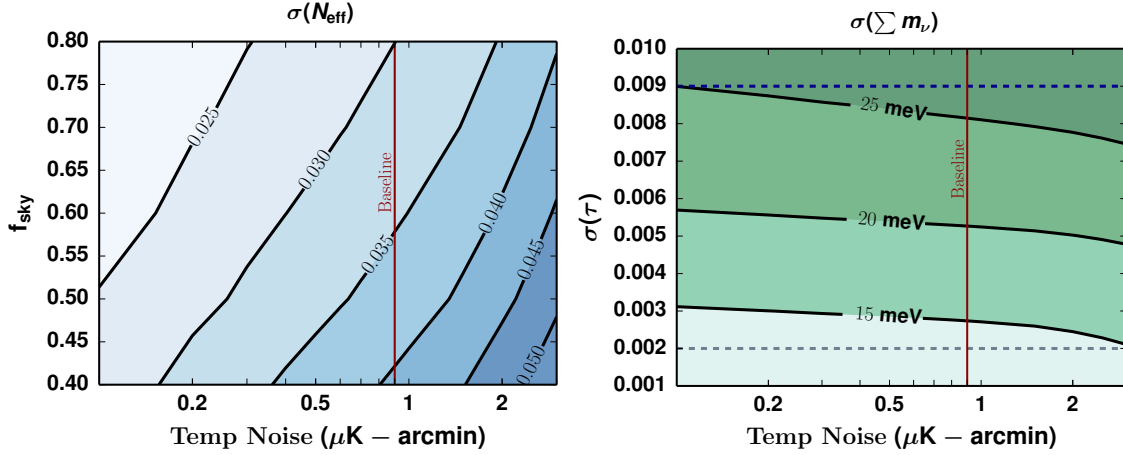
Figure 3: N_{eff} uncertainty as a function of noise and sky fraction (left) and sum of neutrino masses uncertainty as a function of noise and the uncertainty in the measurement of τ, for 0.7 sky fraction (right). The resolution assumed is 5'. Vertical lines denote the expected performance of the baseline mission. The upper blue dashed line is the current *Planck* limit; the lower grey dashed line is the limit from cosmic variance limited measurement of τ. All forecasts assume internal delensing of the T and E-maps [5], including residual non-Gaussian covariances. The $\sum m_\nu$ forecasts include DESI BAO.

dark matter annihilation cross section for dark matter in this mass range.

A particle-independent approach is to constrain dark matter interactions that would affect the evolution of the effective dark matter fluid and its interactions with baryons or photons. The simplest example is to constrain the baryon-dark matter cross section through its effective coupling of the two fluids [6]. These couplings affect the evolution of fluctuations and ultimately the T and E spectra. The current limits of $\sigma \lesssim 10^{-31} - 10^{-34}\,\text{cm}^2 \times (m_{\text{dm}}/\text{MeV})$ can be competitive with direct detection for sub-GeV masses. More exotic dark sectors that include long-range forces can produce an even richer phenomenology in the CMB and in the large-scale structure without necessarily producing an associated signature in direct detection experiments or indirect searches (e.g. [7, 8, 9]).

$\sigma \simeq 10^{-39} - 10^{-35}\,\text{cm}^2$ [**?**].

A host of other physical phenomena including the existence and properties of axions, primordial magnetic fields, and superconducting strings, leave signatures on the spectrum of the CMB and can therefore be constrained by the sensitive measurements of a future Probe [e.g., **? ? ? ? ?**].

Neutrino mass

The origin and structure of the neutrino masses is one of the great outstanding questions about the nature of the Standard Model particles. Measurements of neutrinos in the lab have revealed much about the masses differences and mixing angles. Cosmology compliments the ongoing effort in the lab by offering a measurement of the sum of the neutrino masses, $\sum m_\nu$, through the gravitational influence of the non-relativistic cosmic neutrinos (confirmed by the measurement of N_{eff}). The best current constraint arises from a combination of Planck and BOSS BAO to constraint $\sum m_\nu < 0.12$ eV (95%).

Cosmological measurements are primarily sensitive to the suppression of power on small scales after the neutrinos become non-relativistic, which can be measured via CMB lensing or weak lensing in a galaxy survey. However, these measurements are limited by our knowledge of the primordial amplitude, A_s. In practice, CMB observations most directly constrain $A_s e^{-2\tau}$ and thus

do not provide a high precision measurement of A_s or τ.

Although many surveys hope to detect $\sum m_\nu$, any detection of the minimum value expected from particle physics $\sum m_\nu = 58$ meV at more than 2σ will require a better measurement of τ. The best constraints on τ come from E modes with $\ell < 20$ which require measurements over the largest angular scales. To date, the only proven method for such a measurement is from space. The current limit of $\sigma(\tau) = 0.009$ is from *Planck* [14]. Forecasts for a CMB measurement of $\sum m_\nu$ using the lensing B mode [15] are shown in Figure 3. With the current uncertainty in τ one is limited to $\sigma(\sum m_\nu) \gtrsim 25$ meV; no other survey or cosmological probe would improve this constraint. But PICO will reach the cosmic variance limit of $\tau \sim 0.002$ and will therefore reach $\sigma(\sum m_\nu) < 15$ meV when combined with DESI's measurements of baryon acoustic oscillations [16]. Robustly detecting neutrino mass at $> 3\sigma$ in any cosmological setting is only possible with an improved measurement of τ like the one achievable with PICO.

Using a PICO measurement of τ to achieve $\sigma(\tau) < 15$ meV, implies that either PICO would capable of detecting $\sum m_\nu > 0$ at greater than 4σ or would exclude the inverted hierarchy ($\sum m_\nu > 100$ meV) at 95% confidence, depending on the central value of the measurement.

2.2.2 Cosmic Structure Formation and Evolution (4 pgs. Hill, Battaglia (& Alvarez))

Physics of Reionization

- E-mode power spectrum: τ

- Patchy reionization: kSZ power spectrum and higher-order statistics

- Patchy reionization: quadratic estimator reconstruction

The Sections below need to be rearranged to match other Science Objective(s) from the STM, but to also relay the breadth of science reachable by PICO, even if those goals are not in the STM.

Structure Formation via Gravitational Lensing

- CMB lensing map and auto-power spectrum: figure with signal and quadratic estimator noise curve(s)

- Delensing and neutrino mass constraints assumed to go in fundamental physics chapter

- Cross-correlations: what to focus on here?

- CMB halo lensing: cluster mass calibration

Physics of Galaxy Formation via the Sunyaev-Zel'dovich (SZ) Effects

- Thermal SZ Effect

  - Cluster count forecast

  - y-map and tSZ auto-power spectrum: figure with signal and NILC noise curve(s) [M. Remazeilles]

  - Cross-correlations: forecast S/N with LSST, Euclid, DESI

- Kinematic SZ Effect

- Cross-correlations: forecast S/N with LSST, Euclid, DESI
- Constraints on ICM models: figure with gas pressure and density profile plots, error bars
- Late-time kSZ power spectrum?

2.2.3   Galactic Structure and Star Formation (3 pgs, Chuss & Fissel)

Should address these Science Objectives from the STM:

- "Determine whether the interstellar medium of our galaxy is unique by comparing the ratio of energy in magnetic field to turbulence to that in nearby galaxies."

- "Determine if magnetic fields are the dominant cause of low star formation efficiency in our Galaxy."

- "Determine whether radiative torque is responsible for the alignment of dust grains with magnetic fields"

- "Determine the influence of the magnetic field on Galactic dynamics within the Milky Way."

2.3   Additional Science (2 pgs, de Zotti)

Describe science that we get for free.

2.3.1   Point extragalactic sources in the PICO frequency range

As illustrated by the left panel of Fig. 4, at $\lambda \gtrsim$ few mm the dominant extragalactic population are blazars (flat-spectrum radio quasars, FSRQs, and BL Lacs), typically at $z \gtrsim 1$; the solid blue line shows an example. At shorter wavelengths dusty galaxies take over. The brightest sources in this spectral range are nearby star-forming galaxies like M 61. PICO will also see the brightest high-z sub-mm sources which, due to the "magnification bias", are those whose flux density is boosted by strong gravitational lensing.
Herschel surveys have shown that, at $500\,\mu$m (600 GHz), about 20% of galaxies at the PICO detection limit are strongly lensed (right panel of Fig. 4). This is an extraordinary selection efficiency: for comparison, the fraction of strongly lensed galaxies is of $\sim 10^{-3}$ in all other frequency bands where searches have been carried out. Also, these galaxies have sub-mm colors substantially different from those of the other extragalactic populations and are therefore very easily singled out [**?**].
PICO will detect several thousands strongly lensed galaxies. Objects like the $z = 4$ source HLSJ091828.6 + 514223 (left panel of Fig. 4; [**?**]) would be detectable by PICO up to extreme redshifts ($z > 10$).
The availability of thousands of strongly lensed galaxies opens exciting prospects both on the astrophysical and on the cosmological side (cf., e.g., ref. [**?**]). Compared to searches in other wavebands, PICO detections will extend to much higher redshift sources [most optically-selected strongly lensed galaxies are at $z < 1$, cf. Fig. 7 of ref. **?**] and will pick up the rare most extreme amplifications, thanks to its all sky coverage: the magnification factors, μ, of "*Planck* dusty GEMS" are estimated to be of up to 50 [**?**].
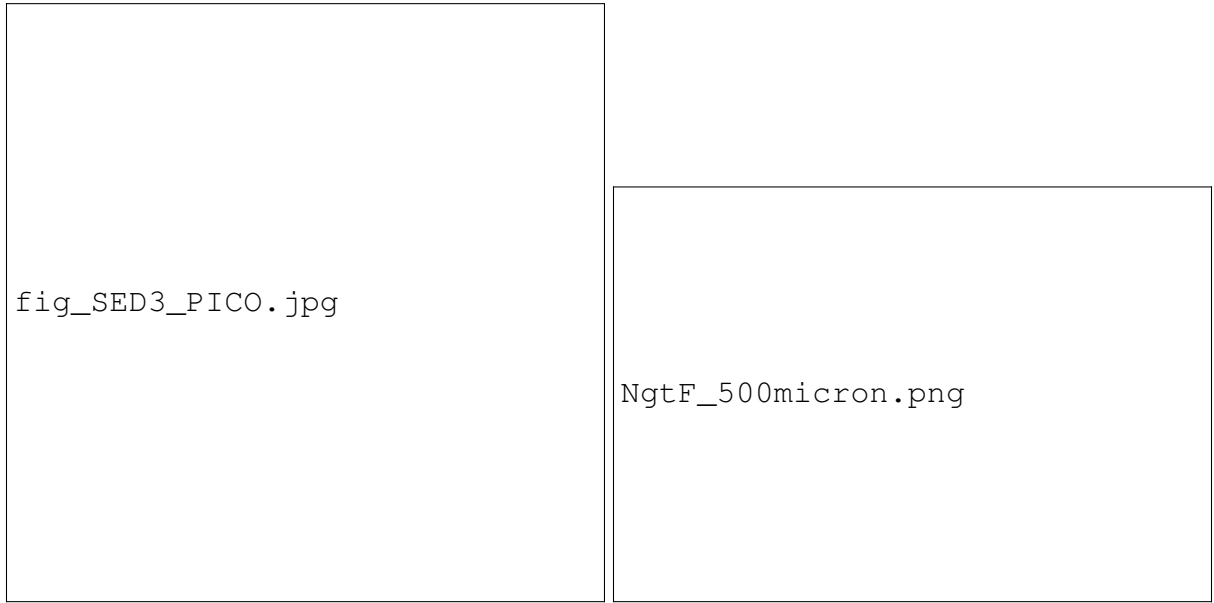
Figure 4: **Left panel.** Examples of SEDs of extragalactic sources detectable by PICO, compared with its point source detection limits (solid black line). The SED of M 61 has been scaled down by a factor of 10. The 90% completeness limits of the Second *Planck* Catalogue of Compact Sources (PCCS2; [**?**]) are also shown. **Right panel.** Integral counts of the various populations of extragalactic sources at $500\,\mu$m as determined by *Herschel* surveys. The vertical red line shows the estimated PICO detection limit.

Figure 5: **Left panel.** SEDs of the cores of two proto-clusters of starbursting galaxies discovered by [?] at $z = 2.41$, by [?] at $z = 2.506$ and by [?] at $z = 4.0$. The first two SEDs include only the contributions of proto-cluster members within $10''$, i.e. over an angular size below the PICO resolution, corresponding to physical radii $\simeq 80\,\mathrm{kpc}$, substantially smaller than the effective proto-cluster sizes. The reported flux densities are therefore lower limits to those that will be measured by PICO. The SED of the 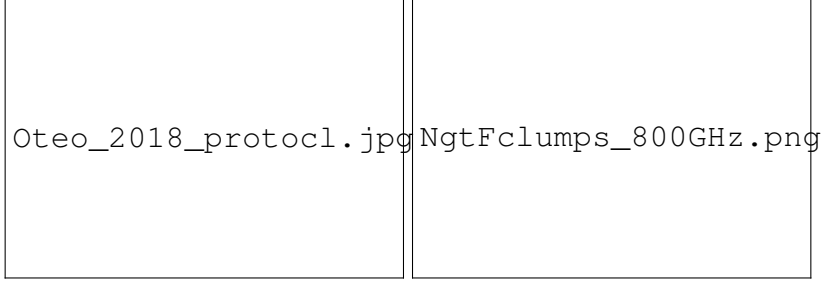$z = 4.0$ proto-cluster correspond to a SFR of $6500\,M_\odot\,\mathrm{yr}^{-1}$, estimated by [?] summing the contributions of galaxies detected by ALMA within a radius of $\simeq 25''$; again this is likely a lower limit to what PICO will measure. The solid black line shows the PICO detection limits. **Central panel.** ALMA image of the $z = 4.0$ proto-cluster discovered by [?], extracted from Fig. 1 of their paper. **Left panel.** Counts of proto-clusters at $800\,\mathrm{GHz}$ predicted by the model of ref. [?]. The vertical red line corresponds to the PICO detection limit.

Sub-mm lensing allows us to probe the most active star-formation phases, hardly visible in the optical. The gravitational flux boosting is accompanied by a stretching of images. Thus follow-up with ALMA can achieve an effective resolution of several milli-arcsec, i.e. can measure galactic structures at $z \simeq 3$ down to the astounding level of $\sim 50 - 60\,\mathrm{pc}$, much smaller than the sizes of Galactic giant molecular clouds [?]. This provides unique direct information on the mechanisms driving the star-formation and on the shapes, sizes and surface brightnesses of star-formation regions.

The detection of several thousands of galaxies at redshifts $\gtrsim 1$ and up to $z > 5$ allows a substantial progress towards a complete census of the dust-enshrouded star-formation history of the universe, i.e. towards tracking the buildup of stellar mass over cosmic time, in particular over epochs of most intense star formation.

The high redshifts of magnified galaxies imply high redshifts of foreground lenses. Optical follow-up will allow us to investigate the total (visible and dark) mass of the lensing galaxies, their density profiles, dark matter sub-structures in a much higher redshift range than in the case of optical selection [?].

Also PICO will explore essentially the entire Hubble volume for the most intense hyperluminous starbursts, testing whether there are physical limits to the star-formation rates of galaxies.

The right panel of Fig. 4 also shows that PICO will detect tens of thousands star forming galaxies in the nearby universe, reaching a surface density about a factor of two higher than that of the IRAS satellite at its $60\,\mu\mathrm{m}$ completeness limit [?]. The IRAS wavebands are relatively insensitive to low temperature dust emission, a significant and largely unexplored component of many nearby galaxies [?]. PICO will provide a full characterization of this component, complementing IRAS data to establish well calibrated dust SEDs as a function of galaxy morphology, luminosity, dust and gas mass, etc..

2.3.2 Early phases of cluster evolution

PICO will open a new window for the investigation of early phases of cluster evolution, when their member galaxies were actively star forming and before the hot IGM was in place. In this phase traditional approaches to cluster detection (X-ray and SZ surveys, searches for galaxy red sequences) work only for the minority of evolved objects; indeed they have yielded only a handful of confirmed proto-clusters at $z \gtrsim 1.5$ [?][1].

SEDs of spectroscopically confirmed sub-mm-bright proto-clusters detectable by PICO are shown in the left panel of Fig. 5). *Planck* has demonstrated the power of low-resolution surveys for the study of large-scale structure [?] but its resolution was too poor to detect individual proto-clusters [?]. As illustrated by the central panel of Fig. 5, the typical sizes of high-z proto-cluster cores are of $\sim 1'$ (cf. also ref. [?]), nicely matching the PICO FWHM at the highest frequencies.

CMB Probe will detect many tens of thousands of these objects (right-hand panel of Fig. 5) up to $z \gtrsim 4$ (left panel). This will allow a real breakthrough in the observational validation of the formation history of the most massive dark matter halos, traced by clusters, a crucial test of models for structure formation. Follow-up observations will characterize the properties of member galaxies, probing the galaxy evolution in dense environments and shedding light on the complex physical processes driving it.

2.3.3 Radio sources

PICO will increase by orders of magnitude the number of blazars selected at sub-mm wavelengths and will determine the SEDs of many hundreds of them up to $800\,\mathrm{GHz}$. The most luminous high-z FSRQs were found to host black holes (BHs) with the largest masses, up to $\sim 4 \times 10^{10}\, M_\odot$ (S5 $0014 + 813$, at $z = 3.366$; see ref. [?]). Such objects have particularly hard mm-wave spectra; thus PICO surveys are well suited to detect them. Objects like S5 $0014 + 813$ are detectable by PICO up to $z > 5$.

Blazar searches are the most effective way to sample the most massive BHs at high z because of the Doppler boosting of their flux densities. Since the flux boosting occurs for jets closely aligned with the line of sight ($\theta < 1/\Gamma$, $\Gamma \sim 15$ being the bulk Lorentz factor), for each FSRQ there are other $2\Gamma^2$ (i.e. hundreds) sources of similar intrinsic properties but pointing elsewhere.

Very large BH masses at high-z challenge models because it is very hard to grow a seed BH from stellar mass to $> 10^9\, M_\odot$ in the limited age of the universe. It is even more so for jetted quasars because jets are likely associated with rapidly spinning BHs whose radiative efficiency is large so that the mass growth is slow. Yet at least 4 FSRQs has been discovered at $z > 5$ (up to $z = 5.48$; [?]). One (SDSS J013127.34032100.1 at $z = 5.18$) has estimated BH mass of $\sim 10^{10}\, M_\odot$ [?].

The PICO surveys of the largely unexplored mm/sub-mm spectral region will also offer the possibility to discover new transient sources [?] or events, such as blazar outbursts.

2.3.4 Source polarization

PICO will make a giant leap forward in the determination of polarization properties of both radio sources and of dusty galaxies over a frequency range where ground based surveys are impractical or impossible. Thanks to its high sensitivity, it will detect in polarization both populations over a

---

[1]More high-z proto-clusters have been found targeting the environment of tracers of very massive halos, such as radio-galaxies, QSOs, sub-mm galaxies. These searches are however obviously biased.

substantial flux density range, determining directly, for the first time, number counts in polarized flux density.

Mm/sub-mm polarimetry of radio sources provides unique information on the magnetic field configuration (geometry and degree of order) in the innermost, unresolved regions of the jets, close to the active nucleus. Polarimetry of dusty galaxies as a function of their inclination is informative on the structure and on the ordering of their large-scale magnetic fields.

2.4 Complementarity with other Measurements and Surveys (1 pg, Lawrence, Schmittfull?)

Should describe complementarity with sub-orbital CMB measurements and with other surveys, both in space and on the ground. This is summary text (more detail in subsections about specific objectives)

2.5 Foregrounds (4 pgs, Jacques and Clem)

The state of knowledge and known challenges; how does PICO address the challenges; forecast of performance.

2.6 Systematic Errors (3 pgs, Crill)

Aside from control of foregrounds, the most compelling reason to observe the CMB from space is the opportunity for excellent control of systematic errors that affect CMB measurements from any platform. The L2 environment offers excellent stability as well as the ability to observe large fractions of the sky on many time scales without interference from the Sun, Earth, or Moon. The redundancy of observations allows the checking of consistency of results and an improved ability to calibrate and to correct systematic errors in post-processing analysis.

As of today, there is a clear path to demonstrate that state-of-the-art technology and data processing can take advantage of the L2 environment and control systematic errors to a level that enables the science goals of PICO.

A rich literature investigates the types of systematic errors due to the environment, the instrumentation, observation strategies, and data analysis that confound the polarization measurement by creating a bias or an increased variance[10, 11, 17]. Every measurement to date has reached a systematic error limit, and have advanced many sophisticated techniques to mitigate systematics, finding both new technological solutions and new analysis techniques. As an example, the BICEP's systematics limited it to r=0.1[?] while through additional effort within the program, BICEP2 achieved a systematics limit of r=6×10^{-3}[18]). In the near term, the ground based and suborbital CMB community will continue to develop new techniques in handling systematics, particularly in developing the CMB-S4 project.

All prior on-orbit measurements of CMB polarization were limited by systematic errors until an in-depth study of the systematics was performed and the post-processing data analysis suppressed them[14, 19, 20]. Paricularly we note Fig. 3 of the Planck legacy paper which indicates Planck's systematic error limits on the polarization power spectral measurements. Recently studied space missions, such as EPIC-IM, LiteBird and *CORE*, have placed systematic error mitigation at the forefront of the case for their mission and have developed tools and strategies for estimating and

mitigating these[21, 22, 23].

End-to-end simulation of the experiment is an essential tool, including realistic instabilities and non-idealities of the spacecraft, telescope, instrument and folding in data post-processing techniques used to mitigate the effects. Systematics are coupled with the spacecraft scan strategy, and the details of the data analysis pipeline.

2.6.1 List of Systematics

The systematic errors faced by PICO can be categorized into three broad categories: 1) Intensity-to-polarization leakage, 2) stability, and 3) straylight and are listed in Table 1. These were prioritized for further study using a risk factor assessed by the working group. The risk factor incorporates the working group's assessment of how mission-limiting the effect is, how well these effects are understood by the community and whether mitigation techniques exist.

The working group's three highest risk systematic errors were studied further and are discussed in subsections below. The PICO team used simulation and analysis tools developed for Planck[24] and *CORE*, adapting them for PICO.

We note that many of the systematics could be mitigated further through the use of polarization modulation such as a half-wave plate or a variable phase delay modulator. For the purposes of the cost constraints of PICO, we investigated mitigation techniques that do not require a modulator.

2.6.2 Absolute polarization angle calibration

The rotation of the CMB polarization can have different causes, including 1. a birefringent primordial Universe, or a Faraday rotation due a primordial magnetic field [28], 2. birefringent foregrounds, or interaction with the Galactic magnetic field, 3. systematic effects in the instrument, and in particular an error on the actual direction of polarization measured by each detector. While the first two sources create a rotation that may depend on scale, position and/or frequency, the latter depends mainly on the detector considered.

A rotation α of the direction of polarization mixes the Q and U Stokes parameters via $Q \pm iU \longrightarrow e^{\mp i2\alpha}(Q \pm iU)$ and thus mixes the the power spectra and their correlations as illustrated in Fig. 6. In Planck, the ground measurements of the detectors orientation had an error of $\pm 0.9^o$ (rel.) $\pm 0.3^o$ (abs.) [30].

The most recent constraints on cosmological birefringence (or systematic rotation) was set in **(author?)** [31], looking for residual signal in TB and EB spectra, but are dominated by the uncertainties on the detector orientations.

For PICO, the relative rotation of the detectors, could be measured with a good accuracy (a few $0.1'$?, †[refs?]†) on the CMB, but the overall rotation is difficult to determine. Known polarized sources, such as the Crab Nebula, could be used to do that but **(author?)** [26] show that the current uncertainty of $0.33^o = 20'$ on the Crab polarization orientation, obtained when combining all the available measurements, would not the measurement of tensorial B modes below $r \sim 0.01$ (assuming everything else to be nominal), far from PICO's target.

Figures **??** and **??** show how the measurement of r by PICO is degraded because of an overall rotation of polarization, and how TB and EB can be used to monitor this rotation, assuming that the only source of polarization rotation is instrumental. These results are obtained assuming the spectra to have a Gaussian likelihood, with a variance $\propto 1/f_{\text{sky}}$, and ignoring the foreground contributions.

Name	Risk	Description	State-of-the-art	Additional Mitigation Needed
Leakage				
Polarization Angle Calibration......................	5	Uncertainty in polarization calibration leaks E→B.	Knowledge of astrophysical calibrators to 0.3°**(author?)** [26]; ground measurement to 0.9° reconstruction to 0.2° using TB and EB demonstrated by *Planck***?**]	See Sect. 2.10.2 for discussion.
Bandpass Mismatch........	4	Edges and shapes of the the spectral filters vary from detector to detector. leaks T → P, P → P if the source's bandpass differs from calibrator's bandpass[**?**]	Precise bandpass measurement[**?**]; SRoll algorithm[**?**]; filtering technique[**?**]; additional component solution (see Banerji& Delabrouille in prep).	State-of-the-art meet requirements.
Beam mismatch	4	Beam shapes differ between detectors that are combined to reconstruct polarization; leaks T → P, P → P	See Sect. 2.10.2	State-of-the-art meet requirements.
Time Response Accuracy and Stability...............	4	Uncertainty of detector in time constants (measurement errors, time variability) biases polarization angle, pointing and beam size. In a constant spin-rate mission (PICO) is degenerate with the beam shape. leaks T→P, P→P	On-orbit reconstruction of time response to 0.1% across a wide signal band[25], residuals corrected as part of beam and map-making algorithm[**?**].	State-of-the-art meet requirements.
Readout Cross-talk.........	4	Power in one detector leaks into other detectors	*Planck*'s high-impedence bolometers with crosstalk measured at the level of 10^{-3} did not impact CMB polarization science[**?**]. Cross-talk low-impedence bolometers measured at XXX.	State-of-the-art meets requirements.
Chromatic beam shape	4	Beam shape is a function of source SED: measured using a planet, used to build a window function to correct CMB power spectrum.	*Planck* simulations and parameterization as part of the likelihood.	Should be further investigated in Phase A of a mission using physical optics simulations.
Gain mismatch	3	Relative gain between detectors that are combined to reconstruct polarization; error leaks T→P	mission-average relative calibration demonstrated to 10^{-4} to 10^{-5} level [**?**]	State-of-the-art measurement of mission-average gain meets requirements; Sect. 2.10.3 describes effects of stability in time in relative gains.
Cross-polarization	3	Q→U rotation by the optical elements of the instrument.	Degenerate with polarization gain calibration.	State-of-the-art meets requirements.
Stability				
Gain Stability	5	Time-variation of detector gain due to time variability of detector heat sink temperature variations and optical loading.	Reconstruction of time variability of gain to 0.2% in *Planck*[**?**].	See Sect. 2.10.3; Gain fluctuations in PICO on the level of XXX% on time scales of YYY can be corrected in post-processing.
Pointing jitter..............	3	Random pointing error mixes T, E and B at small angular scale	Pointing reconstruction in *Planck* to XXX arcsec.	State-of-the-art meets requirements.
Straylight				
Far Sidelobes..............	5	Pickup of Galactic signals at large angles from the main beam axis; Spillover can be highly polarized.	*Planck* validated straylight model in anechoic chamber to -80 dBi[27].	Design of optical system and baffling, informed by telescope straylight simulations. See Sect. 2.10.4 for a study of beams calculated with a physical optics code for the PICO telescope and simulated Galactic pickup during the reference mission.
Other				
Residual correlated cosmic ray hits	3	detectors experience correlated cosmic ray hits below detection threshold resulting in misestimated noise covariance.	*Planck*/HFI found the 5% percent noise correlation due to this effect did not impact results[**?**].	State-of-the-art detector design to reduce cosmic ray cross-section; State-of-the-art analysis techniques (accounting for correlated noise) meet requirements.

Table 1: Systematic errors expected in PICO's measurement of CMB polarization. The risk level was scored from 1 to 5 based on the study team's assessment. Those systematic errors found to be most likely to impact PICO are described further in the text.

In principle, the technique of using the TB and EB spectra can detect and measure a global polarization rotation error at levels ($0.1'$) well below those affecting r measurements in BB ($>$ $1'$). However, a future mission should include additional aspects of the measurements of CMB

Figure 6: Effect of a rotation of the angle of polarization, assuming the Planck 2018 Λ-CDM best fit model [29] and expected PICO noise performance, assuming perfect delensing †[Remove the r=0.01 curve; decide whether to keep beam leakage curve; perhaps remove 60' and 10']†.

polarization, such as delensing, the interaction with foregrounds, and $1/f$ noise in simulating and assessing the impact of an angle calibration error.

2.6.3 Gain Stability

Photometric calibration is the process of converting the raw output of the receivers into a physically-meaningful quantity, such as thermodynamic temperature or brightness. As CMB receivers are usually linear, this process reduces to the characterization of the *gain factor* G:

$$y(t) = G(t) \times T\big(\vec{x}(t)\big) + n(t), \tag{1}$$

where $y(t)$ is the timestream of raw samples produced by the detector, $G(t)$ is the gain factor (which we allow to vary with time), T is the sky temperature observed along direction $\vec{x}(t)$ (which varies with time as the spacecraft spins), and $n(t)$ is a noise term that includes both uncorrelated and correlated noise. It is assumed that the timescale of variation in G ($G/\dot{G}$) is much longer than the typical timescale of variations in T: in the case of Planck, this was of the order of several days. In the case of space CMB experiments, the characterization of $G(t)$ is commonly done using the signal caused by the motion of the spacecraft with respect to the rest frame of the CMB itself. This signal is commonly called the *dipole*, as its most significant contribute is at multipole $\ell = 1$. For the PICO concept study, we evaluated the impact of noise in the estimation of $G(t)$ using the tools developed for the Planck/LFI instrument and the CORE mission proposal. The quality of the estimate depends on the noise level of the receiverse, but also on the details of the scanning strategy. The Planck/LFI experiment, because of a poor choice of the scanning strategy parameters (namely, a too slow precession motion), was forced to avoid using one year out of four in the 2015

data release [REF]. We can anticipate that this problem is not expected in PICO, thanks to the significantly faster precession envisaged.

In order to test the impact of calibration uncertainties, we have run the following analysis:

1. We simulated the observation of the sky, assuming four receivers and the nominal scanning strategy. We included both white noise and $1/f$ noise. The sky only contained CMB anisotropies, plus the CMB dipole.

2. We ran the calibration code to fit the dipole against the raw data simulated during step 1.

3. We simulated again the observation of the sky, but this time we used the values of G computed during step 2, which contain errors due to the presence of $n(t)$ and the CMB signal in Eq. (1). The noise in the output map is therefore the sum of the noise in the error on G and the term n.

The presence of foregrounds in the sky signal would cause a bias in the estimation of the calibration constants, due to the presence of large scale features in the Milky Way at microwave frequencies. A full data analysis pipeline for PICO should pair the calibration step with the component separation step, following a schema similar to what has been done by the Planck/LFI team for the 2018 data release [CITATION]: the application of the calibration code should be followed by a component separation analysis, and these two steps should be iterated until the result converge to a solution. In this analysis we assume to study the calibration at the last iteration, when the components have already been properly separated.

Results of the simulation are shown in Figures XXX and YYY. The scanning strategy employed by PICO allows for a much better calibration than in the case of Planck's, thanks to the much faster precession.

2.6.4 Far Sidelobe Pickup

The main beam (within a few degrees of the axis of beam response) in a CMB mission can be measured to high precision using the planets as compact sources. Measurement of each detector's response to signals more than a few degrees off axis, which tends to be at a very low level (more than –80dB less than the peak response) but spread over a very large solid angle, is difficult to do pre-launch, and may not be done accurately after launch. Nonetheless, this far sidelobe can couple bright Galactic signal from many tens of degrees off-axis and confuse it with polarized signal from the CMB off the Galactic plane.

To evaluate this systematic error, GRASP software[2] was used to compute the PICO telescope's pickup over the full sky. This full-sky beam was convolved with a polarized Galactic signal and a full PICO mission scan using the simulation pipeline. The far sidelibe pickup was estimated to contribute less than XXX to the B-mode angular power spectrum and thus an error in r of YYY.

In a real mission due to the difficulties of measuring this beam, physical optics simulation capabilities must be maintained and validated as well as possible with on-orbit data.

2.6.5 Key Findings

Properly modeling, engineering for, and controlling the effects of systematic errors in a next-generation CMB probe is critical. In particular we note:

---

[2]https://www.ticra.com

- The raw sensitivity of the instrument should include enough margin that data subsets can independently achieve the science goals. This allows testing of the results in the data analysis and additional data cuts, if needed.

- NASA's support of ground-based and suborbital CMB missions will mitigate risk to a future space mission as PICO by continuing to develop analysis techniques and technology for mitigation of systematic errors.

- In a PICO mission's phase A, a complete end-to-end system-level simulation software facility would be developed to assist the team in setting requirements and conducting trades between subsystem requirements while realistically accounting for post-processing mitigation. Any future CMB mission is likely to have similar orbit and scan characteristics to those of PICO, thus there is an opportunity for NASA and the CMB community to invest in further development of this capability now.

2.7 Measurement Requirements (2 pgs, Hanany & Trangsrud)

Some requirements derive from the science (e.g. τ = full sky, r = depth, lensing = resolution) Some requirements derive from foregrounds (e.g. frequency breadth) and some from systematics (e.g. particular scan pattern)

3 Instrument (6 pgs, Hanany & Trangsrud)

Telescope (Hanany / Young), focal plane (Hanany / Young), cooling (Trangsrud), readout (O'Brient) Review: Bock, Hubmayr, Suzuki,

4 Mission (5 pgs, Trangsrud)

To be included: mission architecture, spacecraft and subsystems, orbit, attitude control and determination (Trangsrud)

5 Technology Maturation (4 pgs, O'Brient & Trangsrud)

Requirements, planned activities, schedules and milestones, estimated cost (O'Brient?) For each technology include:

- Requirements

- Planned activities

- Schedule and Milestones

- Estimated Cost

6 Management, Risk, Heritage, and Cost (4 pgs, Trangsrud)

cost, risk, heritage (Trangsrud)

References

[1] G. Steigman. Cosmology confronts particle physics. *Annual Review of Nuclear and Particle Science*, 29:313–338, 1979.
¡¡¡¡¡¡¡ HEAD

[2] M. Bolz, A. Brandenburg, and W. Buchmuller. Thermal production of gravitinos. *Nucl. Phys.*, B606:518–544, 2001. [Erratum: Nucl. Phys.B790,336(2008)].

[3] Christopher Brust, David E. Kaplan, and Matthew T. Walters. New Light Species and the CMB. *JHEP*, 12:058, 2013.

[4] Daniel Baumann, Daniel Green, and Benjamin Wallisch. A New Target for Cosmic Axion Searches. *Phys. Rev. Lett.*, 117(17):171301, 2016.

[5] Daniel Green, Joel Meyers, and Alexander van Engelen. CMB Delensing Beyond the B Modes. *ArXiv e-prints*, 2016.

[6] Cora Dvorkin, Kfir Blum, and Marc Kamionkowski. Constraining Dark Matter-Baryon Scattering with Linear Cosmology. *Phys. Rev.*, D89(2):023519, 2014.

[7] Francis-Yan Cyr-Racine, Roland de Putter, Alvise Raccanelli, and Kris Sigurdson. Constraints on Large-Scale Dark Acoustic Oscillations from Cosmology. *Phys. Rev.*, D89(6):063517, 2014.

[8] Manuel A. Buen-Abad, Gustavo Marques-Tavares, and Martin Schmaltz. Non-Abelian dark matter and dark radiation. *Phys. Rev.*, D92(2):023531, 2015.

[9] Julien Lesgourgues, Gustavo Marques-Tavares, and Martin Schmaltz. Evidence for dark matter interactions in cosmological precision data? *JCAP*, 1602(02):037, 2016. =======

[10] M. Shimon, B. Keating, N. Ponthieu, and E. Hivon. CMB polarization systematics due to beam asymmetry: Impact on inflationary science. *Phys. Rev. D.*, 77(8):083003–+, April 2008.

[11] A. P. S. Yadav, M. Su, and M. Zaldarriaga. Primordial B-mode diagnostics and self-calibrating the CMB polarization. *Phys. Rev. D.*, 81(6):063512–+, March 2010.

[12] Bicep2 Collaboration, P. A. R. Ade, R. W. Aikin, D. Barkats, S. J. Benton, C. A. Bischoff, J. J. Bock, J. A. Brevik, I. Buder, E. Bullock, C. D. Dowell, L. Duband, J. P. Filippini, S. Fliescher, S. R. Golwala, M. Halpern, M. Hasselfield, S. R. Hildebrandt, G. C. Hilton, K. D. Irwin, K. S. Karkare, J. P. Kaufman, B. G. Keating, S. A. Kernasovskiy, J. M. Kovac, C. L. Kuo, E. M. Leitch, M. Lueker, C. B. Netterfield, H. T. Nguyen, R. O'Brient, R. W. Ogburn, IV, A. Orlando, C. Pryke, S. Richter, R. Schwarz, C. D. Sheehy, Z. K. Staniszewski, R. V. Sudiwala, G. P. Teply, J. E. Tolan, A. D. Turner, A. G. Vieregg, C. L. Wong, and K. W. Yoon. Bicep2 III: Instrumental Systematics. *Ap. J.*, 814:110, December 2015.

[13] C. L. Bennett, D. Larson, J. L. Weiland, N. Jarosik, G. Hinshaw, N. Odegard, K. M. Smith, R. S. Hill, B. Gold, M. Halpern, E. Komatsu, M. R. Nolta, L. Page, D. N. Spergel, E. Wollack, J. Dunkley, A. Kogut, M. Limon, S. S. Meyer, G. S. Tucker, and E. L. Wright. Nine-year

Wilkinson Microwave Anisotropy Probe (WMAP) Observations: Final Maps and Results. *The Astrophysical Journal Supplement Series*, 208:20, October 2013. ¿¿¿¿¿¿ reorganizing systematics text

[14] Planck Collaboration, N. Aghanim, M. Ashdown, J. Aumont, C. Baccigalupi, M. Ballardini, A. J. Banday, R. B. Barreiro, N. Bartolo, S. Basak, R. Battye, K. Benabed, J.-P. Bernard, M. Bersanelli, P. Bielewicz, J. J. Bock, A. Bonaldi, L. Bonavera, J. R. Bond, J. Borrill, F. R. Bouchet, F. Boulanger, M. Bucher, C. Burigana, R. C. Butler, E. Calabrese, J.-F. Cardoso, J. Carron, A. Challinor, H. C. Chiang, L. P. L. Colombo, C. Combet, B. Comis, A. Coulais, B. P. Crill, A. Curto, F. Cuttaia, R. J. Davis, P. de Bernardis, A. de Rosa, G. de Zotti, J. Delabrouille, J.-M. Delouis, E. Di Valentino, C. Dickinson, J. M. Diego, O. Doré, M. Douspis, A. Ducout, X. Dupac, G. Efstathiou, F. Elsner, T. A. Enßlin, H. K. Eriksen, E. Falgarone, Y. Fantaye, F. Finelli, F. Forastieri, M. Frailis, A. A. Fraisse, E. Franceschi, A. Frolov, S. Galeotta, S. Galli, K. Ganga, R. T. Génova-Santos, M. Gerbino, T. Ghosh, J. González-Nuevo, K. M. Górski, S. Gratton, A. Gruppuso, J. E. Gudmundsson, F. K. Hansen, G. Helou, S. Henrot-Versillé, D. Herranz, E. Hivon, Z. Huang, S. Ilic, A. H. Jaffe, W. C. Jones, E. Keihänen, R. Keskitalo, T. S. Kisner, L. Knox, N. Krachmalnicoff, M. Kunz, H. Kurki-Suonio, G. Lagache, J.-M. Lamarre, M. Langer, A. Lasenby, M. Lattanzi, C. R. Lawrence, M. Le Jeune, J. P. Leahy, F. Levrier, M. Liguori, P. B. Lilje, M. López-Caniego, Y.-Z. Ma, J. F. Macías-Pérez, G. Maggio, A. Mangilli, M. Maris, P. G. Martin, E. Martínez-González, S. Matarrese, N. Mauri, J. D. McEwen, P. R. Meinhold, A. Melchiorri, A. Mennella, M. Migliaccio, M.-A. Miville-Deschênes, D. Molinari, A. Moneti, L. Montier, G. Morgante, A. Moss, S. Mottet, P. Naselsky, P. Natoli, C. A. Oxborrow, L. Pagano, D. Paoletti, B. Partridge, G. Patanchon, L. Patrizii, O. Perdereau, L. Perotto, V. Pettorino, F. Piacentini, S. Plaszczynski, L. Polastri, G. Polenta, J.-L. Puget, J. P. Rachen, B. Racine, M. Reinecke, M. Remazeilles, A. Renzi, G. Rocha, M. Rossetti, G. Roudier, J. A. Rubiño-Martín, B. Ruiz-Granados, L. Salvati, M. Sandri, M. Savelainen, D. Scott, G. Sirri, R. Sunyaev, A.-S. Suur-Uski, J. A. Tauber, M. Tenti, L. Toffolatti, M. Tomasi, M. Tristram, T. Trombetti, J. Valiviita, F. Van Tent, L. Vibert, P. Vielva, F. Villa, N. Vittorio, B. D. Wandelt, R. Watson, I. K. Wehus, M. White, A. Zacchei, and A. Zonca. Planck intermediate results. XLVI. Reduction of large-scale systematic effects in HFI polarization maps and estimation of the reionization optical depth. *ArXiv e-prints*, May 2016.
¡¡¡¡¡¡¡ HEAD

[15] Manoj Kaplinghat, Lloyd Knox, and Yong-Seon Song. Determining neutrino mass from the CMB alone. *Phys. Rev. Lett.*, 91:241301, 2003.

[16] Michael Levi et al. The DESI Experiment, a whitepaper for Snowmass 2013. *ArXiv e-prints*, 2013.

[17] W. Hu, M. M. Hedman, and M. Zaldarriaga. Benchmark parameters for CMB polarization experiments. *Phys. Rev. D.*, 67:043004–+, February 2003. astro-ph/0210096.

[18] Bicep2 Collaboration, P. A. R. Ade, R. W. Aikin, D. Barkats, S. J. Benton, C. A. Bischoff, J. J. Bock, J. A. Brevik, I. Buder, E. Bullock, C. D. Dowell, L. Duband, J. P. Filippini, S. Fliescher, S. R. Golwala, M. Halpern, M. Hasselfield, S. R. Hildebrandt, G. C. Hilton, K. D. Irwin, K. S. Karkare, J. P. Kaufman, B. G. Keating, S. A. Kernasovskiy, J. M. Kovac,

C. L. Kuo, E. M. Leitch, M. Lueker, C. B. Netterfield, H. T. Nguyen, R. O'Brient, R. W. Ogburn, IV, A. Orlando, C. Pryke, S. Richter, R. Schwarz, C. D. Sheehy, Z. K. Staniszewski, R. V. Sudiwala, G. P. Teply, J. E. Tolan, A. D. Turner, A. G. Vieregg, C. L. Wong, and K. W. Yoon. Bicep2 III: Instrumental Systematics. *Ap. J.*, 814:110, December 2015.

[19] C. L. Bennett, D. Larson, J. L. Weiland, N. Jarosik, G. Hinshaw, N. Odegard, K. M. Smith, R. S. Hill, B. Gold, M. Halpern, E. Komatsu, M. R. Nolta, L. Page, D. N. Spergel, E. Wollack, J. Dunkley, A. Kogut, M. Limon, S. S. Meyer, G. S. Tucker, and E. L. Wright. Nine-year Wilkinson Microwave Anisotropy Probe (WMAP) Observations: Final Maps and Results. *The Astrophysical Journal Supplement Series*, 208:20, October 2013. =======

[20] Planck 2018-I. Planck 2018 results. I. Overview and the Cosmological Legacy of Planck. July 2018. ¿¿¿¿¿¿¿ reorganizing systematics text

[21] M. Hazumi, J. Borrill, Y. Chinone, M. A. Dobbs, H. Fuke, A. Ghribi, M. Hasegawa, K. Hattori, M. Hattori, W. L. Holzapfel, Y. Inoue, K. Ishidoshiro, H. Ishino, K. Karatsu, N. Katayama, I. Kawano, A. Kibayashi, Y. Kibe, N. Kimura, K. Koga, E. Komatsu, A. T. Lee, H. Matsuhara, T. Matsumura, S. Mima, K. Mitsuda, H. Morii, S. Murayama, M. Nagai, R. Nagata, S. Nakamura, K. Natsume, H. Nishino, A. Noda, T. Noguchi, I. Ohta, C. Otani, P. L. Richards, S. Sakai, N. Sato, Y. Sato, Y. Sekimoto, A. Shimizu, K. Shinozaki, H. Sugita, A. Suzuki, T. Suzuki, O. Tajima, S. Takada, Y. Takagi, Y. Takei, T. Tomaru, Y. Uzawa, H. Watanabe, N. Yamasaki, M. Yoshida, T. Yoshida, and K. Yotsumoto. LiteBIRD: a small satellite for the study of B-mode polarization and inflation from cosmic background radiation detection. In *Space Telescopes and Instrumentation 2012: Optical, Infrared, and Millimeter Wave*, volume 8442, page 844219, September 2012.

[22] Christopher G. R. Wallis, Michael L. Brown, Richard A. Battye, and Jacques Delabrouille. Optimal scan strategies for future cmb satellite experiments. *Monthly Notices of the Royal Astronomical Society*, 466(1):425–442, 2017.

[23] P. Natoli, M. Ashdown, R. Banerji, J. Borrill, A. Buzzelli, G. de Gasperis, J. Delabrouille, E. Hivon, D. Molinari, G. Patanchon, L. Polastri, M. Tomasi, F. R. Bouchet, S. Henrot-Versillé, D. T. Hoang, R. Keskitalo, K. Kiiveri, T. Kisner, V. Lindholm, D. McCarthy, F. Piacentini, O. Perdereau, G. Polenta, M. Tristram, A. Achucarro, P. Ade, R. Allison, C. Baccigalupi, M. Ballardini, A. J. Banday, J. Bartlett, N. Bartolo, S. Basak, D. Baumann, M. Bersanelli, A. Bonaldi, M. Bonato, F. Boulanger, T. Brinckmann, M. Bucher, C. Burigana, Z. Y. Cai, M. Calvo, C. S. Carvalho, M. G. Castellano, A. Challinor, J. Chluba, S. Clesse, I. Colantoni, A. Coppolecchia, M. Crook, G. D'Alessandro, P. de Bernardis, G. De Zotti, E. Di Valentino, J. M. Diego, J. Errard, S. Feeney, R. Fernandez-Cobos, F. Finelli, F. Forastieri, S. Galli, R. Genova-Santos, M. Gerbino, J. González-Nuevo, S. Grandis, J. Greenslade, A. Gruppuso, S. Hagstotz, S. Hanany, W. Handley, C. Hernandez-Monteagudo, C. Hervías-Caimapo, M. Hills, E. Keihänen, T. Kitching, M. Kunz, H. Kurki-Suonio, L. Lamagna, A. Lasenby, M. Lattanzi, J. Lesgourgues, A. Lewis, M. Liguori, M. López-Caniego, G. Luzzi, B. Maffei, N. Mandolesi, E. Martinez-González, C. J. A. P. Martins, S. Masi, S. Matarrese, A. Melchiorri, J. B. Melin, M. Migliaccio, A. Monfardini, M. Negrello, A. Notari, L. Pagano, A. Paiella, D. Paoletti, M. Piat, G. Pisano, A. Pollo, V. Poulin, M. Quartin, M. Remazeilles, M. Roman, G. Rossi, J. A. Rubino- Martin, L. Salvati, G. Signorelli, A. Tartari, D. Tramonte, N. Trappe, T. Trombetti, C. Tucker, J. Valiviita,

R. Van de Weijgaert, B. van Tent, V. Vennin, P. Vielva, N. Vittorio, C. Wallis, K. Young, and M. Zannoni. Exploring cosmic origins with CORE: Mitigation of systematic effects. *Journal of Cosmology and Astro-Particle Physics*, 2018:022, April 2018.

[24] Planck Collaboration, P. A. R. Ade, N. Aghanim, M. Arnaud, M. Ashdown, J. Aumont, C. Baccigalupi, A. J. Banday, R. B. Barreiro, J. G. Bartlett, and et al. Planck 2015 results. XII. Full focal plane simulations. *Astron. Astrophys.*, 594:A12, September 2016.

[25] P A R Planck Collaboration: Ade, N Aghanim, C Armitage-Caplan, M Arnaud, M Ashdown, F Atrio-Barandela, J Aumont, C Baccigalupi, A J Banday, R B Barreiro, E Battaner, K Benabed, A Benoît, A Benoit-Lévy, J P Bernard, M Bersanelli, P Bielewicz, J Bobin, J J Bock, J R Bond, J Borrill, F R Bouchet, J W Bowyer, M Bridges, M Bucher, C Burigana, J F Cardoso, A Catalano, A Challinor, A Chamballu, R R Chary, L Y Chiang, H C Chiang, P R Christensen, S Church, D L Clements, S Colombi, L P L Colombo, F Couchot, A Coulais, B P Crill, A Curto, F Cuttaia, L Danese, R D Davies, P de Bernardis, A de Rosa, G de Zotti, J Delabrouille, J M Delouis, F X Désert, J M Diego, H Dole, S Donzelli, O Dore, M Douspis, J Dunkley, X Dupac, G Efstathiou, T A Enßlin, H K Eriksen, F Finelli, O Forni, M Frailis, A A Fraisse, E Franceschi, S Galeotta, K Ganga, M Giard, Y Giraud-Héraud, J González-Nuevo, K M Gorski, S Gratton, A Gregorio, A Gruppuso, J E Gudmundsson, J Haissinski, F K Hansen, D Hanson, D Harrison, S Henrot-Versillé, C Hernandez-Monteagudo, D Herranz, S R Hildebrandt, E Hivon, M Hobson, W A Holmes, A Hornstrup, Z Hou, W Hovest, K M Huffenberger, T R Jaffe, A H Jaffe, W C Jones, M Juvela, E Keihänen, R Keskitalo, T S Kisner, R Kneissl, J Knoche, L Knox, M Kunz, H Kurki-Suonio, G Lagache, J M Lamarre, A Lasenby, R J Laureijs, C R Lawrence, R Leonardi, C Leroy, J Lesgourgues, M Liguori, P B Lilje, M Linden-Vørnle, M López-Caniego, P M Lubin, J F Macías-Pérez, C J MacTavish, B Maffei, N Mandolesi, M Maris, D J Marshall, P G Martin, E Martínez-González, S Masi, S Matarrese, T Matsumura, F Matthai, P Mazzotta, P McGehee, A Melchiorri, L Mendes, A Mennella, M Migliaccio, S Mitra, M A Miville-Deschênes, A Moneti, L Montier, G Morgante, D Mortlock, D Munshi, J A Murphy, P Naselsky, F Nati, P Natoli, C B Netterfield, H U Nørgaard-Nielsen, F Noviello, D Novikov, I Novikov, S Osborne, C A Oxborrow, F Paci, L Pagano, F Pajot, D Paoletti, F Pasian, G Patanchon, O Perdereau, L Perotto, F Perrotta, F Piacentini, M Piat, E Pierpaoli, D Pietrobon, S Plaszczynski, E Pointecouteau, A M Polegre, G Polenta, N Ponthieu, L Popa, T Poutanen, G W Pratt, G Prézeau, S Prunet, J L Puget, J P Rachen, M Reinecke, M Remazeilles, C Renault, S Ricciardi, T Riller, I Ristorcelli, G Rocha, C Rosset, G Roudier, M Rowan-Robinson, B Rusholme, M Sandri, D Santos, A Sauvé, G Savini, E P S Shellard, L D Spencer, J L Starck, V Stolyarov, R Stompor, R Sudiwala, F Sureau, D Sutton, A S Suur-Uski, J F Sygnet, J A Tauber, D Tavagnacco, L Terenzi, M Tomasi, M Tristram, M Tucci, G Umana, L Valenziano, J Valiviita, B Van Tent, P Vielva, F Villa, N Vittorio, L A Wade, B D Wandelt, D Yvon, A Zacchei, and A Zonca. Planck 2013 results. VII. HFI time response and beams. *arXiv.org*, pages 1–31, March 2013.

[26] Jonathan Aumont, Juan-Francisco Macias-Perez, Alessia Ritacco, Nicolas Ponthieu, and Anna Mangilli. Absolute calibration of the polarisation angle for future CMB B-mode experiments from current and future measurements of the Crab nebula. May 2018.

[27] J A Tauber, H U Nørgaard-Nielsen, P A R Ade, J Amiri Parian, T Banos, M Bersanelli, C Burigana, A Chamballu, D de Chambure, P R Christensen, O Corre, A Cozzani, B Crill,

G Crone, O D'Arcangelo, R Daddato, D Doyle, D Dubruel, G Forma, R Hills, K Huffenberger, A H Jaffe, N Jessen, P Kletzkine, J M Lamarre, J P Leahy, Y Longval, P de Maagt, B Maffei, N Mandolesi, J Martí-Canales, A Martín-Polegre, P Martin, L Mendes, J A Murphy, P Nielsen, F Noviello, M Paquay, T Peacocke, N Ponthieu, K Pontoppidan, I Ristorcelli, J B Riti, L Rolo, C Rosset, M Sandri, G Savini, R Sudiwala, M Tristram, L Valenziano, M van der Vorst, K van 't Klooster, F Villa, and V Yurchenko. Planckpre-launch status: The optical system. *Astronomy and Astrophysics*, 520:A2, September 2010.

[28] Levon Pogosian and Alex Zucca. Searching for primordial magnetic fields with CMB B-modes. *Classical and Quantum Gravity*, 35(12):124004, May 2018.

[29] Planck 2018-VI. Planck 2018 results. VI. Cosmological parameters. July 2018.

[30] C. Rosset, M. Tristram, N. Ponthieu, P. Ade, J. Aumont, A. Catalano, L. Conversi, F. Couchot, B. P. Crill, F.-X. Désert, K. Ganga, M. Giard, Y. Giraud-Héraud, J. Haïssinski, S. Henrot-Versillé, W. Holmes, W. C. Jones, J.-M. Lamarre, A. Lange, C. Leroy, J. Macías-Pérez, B. Maffei, P. de Marcillac, M.-A. Miville-Deschênes, L. Montier, F. Noviello, F. Pajot, O. Perdereau, F. Piacentini, M. Piat, S. Plaszczynski, E. Pointecouteau, J.-L. Puget, I. Ristorcelli, G. Savini, R. Sudiwala, M. Veneziani, and D. Yvon. Planck pre-launch status: High Frequency Instrument polarization calibration. *A&A*, 520:A13+, September 2010.

[31] Planck collaboration. Planck intermediate results. XLIX. Parity-violation constraints from polarization data. *Astronomy and Astrophysics*, 596:A110, December 2016.